Metabolomics reveals highly regional specificity of cerebral sexual dimorphism in mice

Floris Chabrun, Xavier Dieu, Guillaume Rousseau, Stéphanie Chupin, Franck Letournel, Vincent Procaccio, Dominique Bonneau, Guy Lenaers, Gilles Simard, Delphine Mirebeau-Prunier, et al.

Metabolomics Reveals Highly Regional Specificity of Cerebral Sexual Dimorphism in Mice

Short Title:

Brain sexual dimorphism

Authors:

Floris Chabrun[1,2], Xavier Dieu[1,2], Guillaume Rousseau[1,2], Stéphanie Chupin[1], Franck Letournel[3,4], Vincent Procaccio[1,2], Dominique Bonneau[1,2], Guy Lenaers[2], Gilles Simard[1], Delphine Mirebeau-Prunier[1,2], Juan Manuel Chao de la Barca[1,2], Pascal Reynier[1,2]*

Affiliations:

[1]Département de Biochimie et Génétique, Centre Hospitalier Universitaire d'Angers, France

[2]Equipe Mitolab, Unité Mixte de Recherche MITOVASC, CNRS 6015, INSERM U1083, Université d'Angers, Angers, France

[3]Laboratoire de Neurobiologie et Neuropathologie, Centre Hospitalier Universitaire d'Angers, France

[4]Unité Mixte de recherche MINT, CNRS 6021, INSERM 1066, Université d'Angers, Angers, France

*Correspondence to:

Pascal Reynier, MD, PhD, Département de Biochimie et Génétique, Centre Hospitalier Universitaire, F-49933, Angers, France. Email: pareynier@chu-angers.fr

Abstract

The development of personalized medicine according to gender calls for the integration of sexual dimorphism in pre-clinical models of diseases. Although sexual dimorphism in the brain of the mouse has been the subject of several behavioral, neuroimaging and experimental studies, very few have characterized the bases of sexual dimorphism in the brain on the omics scale. In particular, physiological variations in metabolomic and lipidomic terms related to gender have not been mapped in the brain. We carried out a metabolomic analysis, targeting 188 metabolites representative of various cellular structures and metabolisms, in three brain regions: frontal cortex, brain stem and cerebellum, in 3-month-old C57BL-6J male (n=20) *vs*. female (n=20) mice. Our results demonstrate the existence of sexual dimorphism in the whole brain as well as in separate brain regions. Half of the 129 accurately measured metabolites were involved in the sexual dimorphism of the murine brain, but only 8% of those (hydroxyproline, creatinine, hexoses, tryptophan, threonine and lysoPC.a.C18.2) were involved in common in the three cerebral regions, while 71%, including phosphatidylcholines, lysophosphatidylcholines, sphingomyelins, acylcarnitines, amino acids, biogenic amines, and polyamines, were specific to only one region of the brain, underscoring the highly regional specificity of cerebral sexual dimorphism in mice.

Keywords

Brain; sex dimorphism; metabolomics

Abbreviations

QC: Quality Controls; PCA: Principal Components Analysis; PLS-DA: Projection to Latent Structures-Discriminant Analysis; OPLS-DA: Orthogonal Projection to Latent Structures-Discriminant Analysis; $Q2_C$: Cumulated Q-squared value; VIP: Variable Importance in Projection

Introduction

Despite important differences between male and female physiology, animal studies on males were still, until recently, largely dominant [1], generating considerable bias when the data were transposed to females in view of medical applications [2]. In particular, a gender imbalance may constitute a drawback for therapeutic studies, considering that responses to drugs may vary greatly according to sex [3]. For instance, the withdrawal of 80% of the drugs from the US market is due to the increased risk of therapeutic accidents in women [4]. Thus, the US National Institutes of Health now recommends that an increasing proportion of pre-clinical studies should be performed on cellular and animal models of both sexes [5,6]. Contrary to common belief, the sex-related variability could be paradoxically even greater in males than in females, as recently shown by the comparison of the variance of 142 phenotypic traits in male and female rats [7].

Metabolomics offers a global and integrated view of sexual dimorphism. Indeed, metabolomic studies performed on samples of plasma, serum or urine, from the human, the pig, or the rat, or on the whole organism, such as the drosophila, have already revealed the far-reaching influence of sex on the metabolism [8–12]. For instance, the analysis of sera from more than 3000 individuals has revealed 102 metabolites that vary according to sex, thus providing the first model of the metabolic architecture of human serum [13], highlighting several metabolic pathways affected by sex, such as those of energetic substrates [14], the composition of phospholipids [15], and oxidative stress [16].

However, most of the knowledge acquired on the metabolomics of sexual dimorphism was obtained from studies of biological fluids, whereas organs have been poorly explored, thus posing a serious challenge for deciphering the systemic cartography of sexual metabolomics in normal and pathological organs of animal models. For instance, in a mouse model of inherited optic neuropathy that we recently explored using targeted metabolomics, sexual influence in the plasma and optic nerve metabolomes was at least as important as that related to the mutation causing the disease, and the biochemical phenotype was notably influenced by sex [17,18].

Brain imaging studies, especially those using magnetic resonance imaging (MRI), show gender-based differences both at the structural and functional levels in animal models [19,20] as well as in humans [21,22]. MRI analysis of some 1400 human brains revealed high

variability with an extensive overlap between females and males regarding the distribution of gray matter, white matter and connections, showing that the human brain cannot be sorted into two distinct classes, typical of males or females but viewed rather as a continuum [23]. Epigenetics [24] and gene expression [25] analyses also showed sharp gender-specific differences [26]. For instance, among 4508 genes analyzed, 612 genes (13.6%) presented a dimorphic expression in the mouse [27], but the metabolomic cartography of sexual dimorphism in the brain under healthy physiological conditions has not been documented yet.

In this study we have investigated sex-related metabolic differences in three brain regions of young wild-type adult mice, i.e. the frontal cortex, brain stem and cerebellum, using a highly standardized targeted metabolomics approach.

Materials and Methods

Analytical workflow (Fig. 1.A)

All the experiments were performed in accordance with the European Community Guiding Principles for the care and use of animals (Directive 2010/63/UE; Décret n°2013-118). Twenty wild-type female and twenty wild-type male *Mus musculus* C57BL-6J (B6) mice were born and bred in identical conditions in the same animal housing facilities, until the age of 3 months. Animals were housed at constant temperature (22 ± 2°C) and humidity (55 ± 20%) with a 12-hour light/dark cycle, with free access to food (SAFE A04, SAFE, Augy, France) and water (public water supply). They were subjected to a 12-hour fast before autopsies that were randomly conducted, to avoid batch-effect variations, between 9 and 12 am over 4 consecutive days, to avoid variability due to the circadian rhythm. After a short exposition (45 sec) to isoflurane 3%, the mice were decapitated, their brain extracted and separated into the three regions of interest: the frontal cortex, brain stem and cerebellum. In order to limit the post-mortem alteration of the metabolome, we chose these three brain regions with clear anatomical distinctions that allowed rapid dissection within a few minutes. Decapitation after isoflurane anesthesia was chosen in order to minimize the metabolic impact on the tissues [28]. The samples were immediately plunged into liquid nitrogen before their conservation at -80°C until the extraction of metabolites.

Before extraction, the samples were weighed using an XA105DU analytical balance (Mettler Toledo, Viroflay, France) with an accuracy of 0.01 mg. Tissue samples were collected in pre-cooled (dry ice) 2.0 ml homogenization Precellys tubes prefilled with 1.4 mm diameter

ceramic beads and 3 µl/mg cold methanol [29]. Tissues were homogenized by two grinding cycles, each at 6600 rpm for 20 seconds, spaced 20 seconds apart, using a Precellys homogenizer (Bertin Technologies, Montigny-le-Bretonneux, France) kept at +4ºC. The supernatant was recovered after centrifuging the homogenate and kept at -80ºC until mass spectrometric analysis. Technical issues encountered during extraction led to the loss of three samples so that thus the final number of samples analyzed was 39, 40, and 38 for the brain stem, cerebellum, and frontal cortex, respectively.

Targeted quantitative metabolomic analysis was carried out as described by Chao de la Barca et al. [30], using the Biocrates® Absolute IDQ p180 kit (Biocrates Life sciences AG, Innsbruck, Austria). This kit uses mass spectrometry (QTRAP 5500, SCIEX, Villebon-sur-Yvette, France) to quantify 188 different molecules. Flow injection analysis coupled with tandem mass spectrometry (FIA-MS/MS) was used to analyze carnitine, acylcarnitines, lipids and hexoses, whereas liquid chromatography was used to separate amino acids and biogenic amines before quantitation using mass spectrometry (LC-MS/MS). To prevent batch-effect variations, all samples of the same tissue were run using the same kit with a random distribution of male and female samples over the plate. Peaks were integrated in order to retrieve raw data as a matrix compiling the concentrations of the 188 metabolites for the 117 samples, in addition to the calibration samples and quality control values. Three quality controls (QCs) composed of three concentrations of human plasma samples, i.e. low (QC1), medium (QC2) and high (QC3), were used to evaluate the performance of the analytical assay. A seven-point serial dilution of calibrators was used to generate calibration curves for the quantification of amino acids and biogenic amines.

A cleaning step was performed to filter unusable data: metabolites with more than 30% of values lying outside the ~~quantification~~ detection limits were removed from the datasets. For all features withdrawn in this manner, a Chi-squared test was performed between the number of values within bounds and out-of-bounds in males and females, to prevent removal of discriminant features, i.e. features with a significant gender difference and those within or out-of-range of the distribution. Three separate datasets were then independently processed: row sum normalization, fold-change calculation for each compound, and matrix centering and scaling, to ensure statistical comparability between metabolites and individuals. These datasets were then independently processed through the statistical workflow. In parallel, these

three datasets were pooled into a global dataset, which was processed in the same way as any of the three separated datasets.

Statistical workflow (Fig. 1.B)

Each dataset was analyzed using both the unsupervised and supervised approaches. Principal Components Analysis (PCA), an unsupervised approach, was used to identify outliers and spontaneous clusters.

Supervised modeling was then used to discriminate between the samples by either gender or type of tissue from the global dataset. The dataset was partitioned into a training set and a test set, with a ratio ranging from 80/20% (global dataset) to 66/33% (separate datasets), retaining at least 12 samples in each test set. This partition was performed randomly, with respect to the original distribution of gender and type of tissue. Models were challenged with the training set, while the test sets were used to assess the prediction quality of the models to prevent over-fitting. Orthogonal Projection to Latent Structures-Discriminant Analysis (OPLS-DA) was used for gender prediction. Since OPLS-DA is not suited for multi-class predictions, Projection to Latent Structures-Discriminant Analysis (PLS-DA) modeling was used for tissue prediction [31]. The robustness of both the PLS-DA and OPLS-DA models was assessed with the cumulated Q-squared value ($Q2_C$), and by determinations of specificity (Sp) and sensitivity (Se). The value of $Q2_C$ varies from 0 to 1, with a higher $Q2_C$ reflecting a higher quality model. The minimal threshold for $Q2_C$ was set at ≥ 0.4 to ensure models with reasonably good quality [31]. Due to the small number of samples in the test set, the sensitivity and specificity thresholds for the predictions with the test sets were set at 1.0 (i.e. perfect predictions). The importance of each feature regarding gender or tissue discrimination was then assessed by retrieving the Variable Importance in Projection (VIP) of each compound for each model. Compounds with a VIP higher than 1 were considered highly important for gender or tissue prediction [32]. Metabolites were then compared using either VIP or fold-change for gender prediction, or VIP and mean concentration per tissue for tissue prediction. All the data processing, statistical analysis, and graphical work were carried out using the R software (version 3.4.1, 64-bit) [33]. PCA values were computed using the FactoMineR R package (version 1.39) [34]. The PLS-DA and OPLS-DA models were computed using the Bioconductor ropls R package (version 1.10.0) [35]. Image manipulation and formatting were performed using GNU Image Manipulation Program (GIMP) software (version 2.10).

Results

Global dataset

Supplementary Table 1 shows the raw data collected. Of the 188 metabolites analyzed, 102 were accurately measured in each of the 117 samples taken from the three brain tissues studied, i.e. the frontal cortex, brain stem and cerebellum. Data were first analyzed from a global point of view with Principal Components Analysis (PCA) to identify the differences between the three tissues, and between sexes in the sum of the three tissues. The first four principal components of this global PCA model showed the spontaneous clustering of each tissue and sex **(Fig. 2)**. Samples were well separated according to tissue on the first plan **(Fig. 2.A)** with the first two principal components comprising 41.6% and 21.9% of the variance between the samples, respectively, and partially by the third dimension **(Fig. 2.B)** comprising 14.4% of the total variance. Only the fourth principal component showed samples clustering by gender **(Fig. 2.D)**, involving only 3.8% of the variance. Thus, this PCA showed that regional differences were largely predominant, compared to sexual dimorphism.

Differences between tissues and sexes among the 117 samples were assessed using the metabolites with a high positive or negative correlation (Absolute value of Pearson's correlation coefficient $|r| > 0.80$) with the first four principal components. These differences were mainly due to phosphatidylcholines and sphingomyelins (high positive correlation with the 1st and 2nd principal components) and spermidine (high negative correlation with the 2nd principal component). Cerebellums were separated from the other two tissues by the 3rd principal component, with lower values of asparagine and alanine, and higher values of acylcarnitines C2, C3 and free carnitine C0. The full list of compounds and their correlation factors with the 1st to the 4th principal components is shown in **Supplementary Table 2**. Although the 4th principal component clustered samples by gender, no compounds had a high positive or negative correlation ($|r| > 0.8$) with this principal component. This indicates that, even though there may be a genuine sexual dimorphism, its complexity throughout the brain is such that it is difficult to grasp from a global point of view.

Both Projection to Latent Structures-Discriminant Analysis (PLS-DA) (tissue prediction) and Orthogonal Projection to Latent Structures-Discriminant Analysis (OPLS-DA) (gender prediction) supervised models attained high accuracy on the whole dataset, with $Q2_C$ (Q-squared value) values of 0.965 and 0.816, respectively, and perfect prediction on the test set. **Supplementary Fig. 1** shows the score plots for the models.

PLS-DA and OPLS-DA variable importance in projection (VIP) scores for each metabolite were used to assess the importance of each compound in predicting either the tissue or gender of each sample. For tissue prediction, compounds with a VIP higher than 1 were represented on a Kiviat diagram **(Fig. 3).** These results confirmed those previously obtained with the PCA. Indeed, most phosphatidylcholines showed higher levels in the brain stem and cerebellum compared to the frontal cortex. In addition, most amino acids, including alanine, asparagine and glutamine, were at higher concentrations in the frontal cortex compared to the other two tissues. Glycine had a higher concentration in the brain stem, while acylcarnitines C0, C2 and C3 had higher levels in the cerebellum compared to the frontal cortex and the brain stem.

For gender prediction, compounds with a VIP higher than 1 were represented on a volcano plot **(Fig. 4.A)** and a word cloud, allowing a more convenient visualization of the same information **(Fig. 4.B)**. On the volcano plot, compounds were positioned according to their VIP (y-axis) and loadings (i.e. logarithm to the base 2 of $\frac{male}{female}$ fold-change) (x-axis). On the word cloud, compounds were placed with a label size set according to their VIP, and colored according to their loadings. Compounds in deep blue have higher values in females, while compounds in deep red have higher values in males. The most discriminant metabolites were trans-4-hydroxyproline, sum of hexoses, tyrosine and lysophosphatidylcholine C18:2 with higher concentrations in males, and threonine and tryptophan with higher concentrations in females.

Separate datasets

PCA results are not presented since, regardless of the tissue, PCA first plans were not sufficient to separate males from females. Furthermore, no notable outliers were detected on PCA. OPLS-DA score plots for the models are presented in **Supplementary Fig. 2**.

However, the supervised OPLS-DA models showed $Q2_C$ of 0.837, 0.657 and 0.467 for the brain stem, frontal cortex and cerebellum, respectively. All models showed 100% sex prediction accuracy on the test sets (sensitivity: Se = 1, specificity: Sp = 1).

For each tissue, the OPLS-DA results are presented in the form of both a volcano plot and a word cloud on **Fig. 5**. Only compounds with a VIP greater than 1 are represented on these plots. Compared to the global analysis discussed above, these results confirmed the higher levels, in males *vs*. females, of trans-4-hydroxyproline in all three brain regions explored. The

sum of hexoses, lysophosphatidylcholine C18:2 and creatinine also showed higher values in males compared to females in the three brain regions. Threonine and tryptophan showed higher values in females than in males in the three tissues. The full list of compounds with their VIPs for gender discrimination in the brain stem, frontal cortex and cerebellum is shown in **Supplementary Table 3**. Besides the differences already highlighted by the global analysis, most compounds showed sexual dimorphism specific to either one or two brain regions.

For the OPLS-DA prediction of gender, a Venn diagram was constructed to assess sex-specific differences common to the three brain regions studied or specific to only one or two of these regions **(Fig. 6)**. Features were placed in each brain region circle if their VIP for gender prediction for this tissue was higher than 1. Among the compounds dosed in this study, the brain stem showed the highest sexual dimorphism with 51 metabolites having a VIP higher than 1. The frontal cortex and the cerebellum showed 24 and 25 compounds with a VIP higher than 1, respectively.

Discussion

To explore the cerebral sexual dimorphism of the most frequently used research animal species to mimic human diseases, e.g. the mouse, we used a highly standardized, quantitative metabolomics and lipidomics approach to explore a whole subset of 129 molecules representative of various structures and metabolic pathways. The global unsupervised PCA approach showed that the metabolic heterogeneity between the three brain regions explored was largely predominant compared to the variability caused by gender, the sexual dimorphism being clearly demonstrated by the supervised approach. As shown in **Fig. 6**, among the 73 metabolites showing the sexual dimorphism, only six (8%) were common to the three brain regions, while three to eight were common to two brain regions, and 52 (71%) were specific of only one brain region, thus revealing a large regional variation of the cerebral metabolic sexual dimorphism.

Regional metabolomic variations independent of gender

The brain stem and cerebellum were mostly characterized by higher levels of phosphatidylcholines; the frontal cortex by increased amino acid levels, mostly alanine, asparagine and glutamine; the cerebellum by lower concentrations of asparagine and alanine, and higher values of free carnitine, and C2 and C3 acylcarnitines; finally, the brain stem by

higher glycine levels. An earlier metabolomic study performed on six brain regions from six FVB/N mice (three males and three females) also evidenced specific profiles for each brain region using another set of 85 polar metabolites [36]. The most discriminant metabolites for brain regional specificity in this study were glycine, as in our study, and 5-oxoproline, pyrophosphoric acid, taurine, 2-hydroxypyridine, phosphoethanolamine, hydrogen sulfide, dopamine and glycerol.

Most sex-discriminant metabolites in the brain are hormonally influenced

Bovo et al. used a similar targeted metabolomics approach to characterize the metabolome in the plasma of the pig by comparing castrated males to gilts (young females) [9]. They identified 85 metabolites contributing to the differences between the two groups of pigs. These metabolites include free carnitine and acylcarnitines (n=10), phosphatidylcholines (n=40), lysophosphatidylcholines (n=5), sphingomyelins (n=8), hexoses (sum of), amino acids (n=12), and biogenic amines (n= 9), indicating that most of the sex-discriminant metabolites that we found in the brain are influenced by sexual hormones.

Functional projection of metabolic variations

Fig. 7 summarizes the key metabolites found to be dimorphic in the mouse brain, as well as the biological functions that may be impacted by these variations. The link between metabolites and biological functions is detailed below.

The phospholipidic signature of brain sexual dimorphism

Phosphatidylcholines are composed of a choline head group, a glycerophosphoric acid and two fatty acids of different sizes. These are the commonest lipids in tissues, mostly in cell membranes, accounting for 40-65% of the dry brain weight [37]. Among the 76 phosphatidylcholines measured, 32 (42%) were involved in the sexual dimorphism of the brain with major regional variations. This dimorphism was highly predominant in the brain stem, suggesting sexual differences in the composition of cellular membranes. By providing the choline moiety, phosphatidylcholines are also precursors of acetylcholine [38], a neurotransmitter and a neuromodulator involved in the processes of arousal, attention, memory and motivation. Interestingly, a global increase of the phosphatidylcholine concentration in the plasma of women has already been reported [13,39], and these phospholipids are known to be regulated by sexual hormones [9].

Lysophosphatidylcholines are hydrolytic products of phosphatidylcholines mediated by phospholipases A2 or A1. Among the 14 lysophosphatidylcholines measured, five (35%) were affected by gender with regional differences. Interestingly, lysoPC.a.C18:2, the only lysophosphatidylcholine found dimorphic in all three brain regions, was also one of the most significantly increased lysophosphatidylcholines found in the serum from men compared to that from women [13]. In the brain, lysophosphatidylcholines are powerful inducers of myelin sheath phagocytosis through the recruitment of macrophages and microglia [40].

Sphingomyelins are composed of a phosphocholine head group, a sphingosine, and a fatty acid of variable size. They are found in the plasma membranes and are abundant in the myelin sheath, where they contribute to the insulation of axons. Among the 15 sphingomyelins measured, eight (53%) were involved in sexual dimorphism with regional differences. Interestingly, in the brain stem, the sharp increase of phosphatidylcholines in females was accompanied by an increase of the seven dimorphic sphingomyelins. Increased concentration of sphingomyelins has also been found in sera from women [13].

The cerebral sexual dimorphism of energetic metabolism

Taken together, the concentrations of hexoses, acylcarnitines and creatinine showed an high sexual dimorphism of the energetic metabolism with a regional specificity for acylcarnitines. The increased level of hexoses in the three brain regions of males was one of the strongest contributors to the sexual signature. The expression of glucose transporters in mice, including GLUT class I and SGLT, is known to be gender-specific [41]. Furthermore, the glucose-dependent energy production in the rat is higher in females than in males because of greater pyruvate dehydrogenase activity [42], and positron emission tomography in humans has also revealed higher overall cerebral glucose metabolism in females than in males [43]. Thus, the lower consumption of glucose in males compared to that in females could explain its relative accumulation.

Acylcarnitines are the activated form of fatty acids, allowing their mitochondrial oxidation. Among the 40 acylcarnitines measured, only four (10%) contributed to the sexual dimorphism. Energy production in the brain is predominantly glucose-dependent, explaining the fact that acylcarnitines are not massively involved in cerebral sexual dimorphism.

Nevertheless, the fact that hexoses are globally increased in males and acylcarnitines in females reflects subtle differences in the consumption of energetic substrates in the brain. Sexual dimorphism of acylcarnitines has already been reported in rat plasma [44], liver, heart and skeletal muscle [45], and in human plasma [39] and urine [35].

Creatinine is the degradation product of creatine, not measured here, which is involved in the phosphocreatine system mediating ATP storage and ADP/ATP exchanges. Creatinine was increased in all three regions of the male brain. It is also possible that the higher whole-body skeletal muscle mass in males may raise creatinine levels, as discussed below for hydroxyproline.

The amino-acid signature of cerebral sexual dimorphism

Trans-4-hydroxyproline (t4.OH.Pro) shows the highest sexual dimorphism all through the brain, with higher values in males than in females in the three regions of the brain studied. Hydroxyproline is generated by the hydrolysis of collagen, the mass of which is consistently higher in males [46,47], particularly in the bones and muscles [48]. Higher hydroxyproline levels in the male brain may either reflect this higher muscle and bone mass, or preferentially the faster collagen turnover due to increased bone resorption. At present, hydroxyproline represents the most distinctive feature of the sexual dimorphism in mouse brain, with positive and negative predictive values ≥ 0.9. Proline also showed higher levels in males but only in the brain stem and frontal cortex. In addition to its peculiar richness in collagens, this amino acid also plays physiologic roles in neuromodulation [49] and in the biosynthesis of glutamate, an excitatory neurotransmitter [50].

Serine, glycine, threonine, and lysine show similar sexual profiles. Glycine showed both regional and sexual variations. As already known, its concentration was higher in the brain stem than in the other regions of the brain [51]. It was higher in the male brain stem but lower in the cerebellum. Together with glutamate, glycine is known to be one of the major inhibitory neurotransmitters in the brain [51]. Serine, a direct precursor of glycine, was also at higher levels in the cerebellum of female mice. Interestingly, targeted metabolomic analysis of the sera from 3,300 individuals, showed that glycine and serine levels were significantly lower in males (-14%) than in females whereas the concentrations of most of the other amino acids were higher in males [13]. Threonine, also a precursor of glycine, was at higher levels in

all three cerebral regions in females. ~~The concentrations of threonine were correlated with those of glycine in the cortex and the brain stem, the increased level of threonine in the plasma leading to the increased concentration of glycine in the brain, thereby affecting the equilibrium of the neurotransmitter [52].~~

Lysine, also at a greater concentration in the cerebellum of female mice, is mainly degraded by the L-pipecolate pathway in the brain [53,54] and higher levels of L-pipecolate have already been evidenced in the cerebellum [54]. One of the intermediate products in this pathway is Δ^1-piperideine-2-carboxylate (P2C), which plays a key role in brain development, metabolism, electrophysiology, and regulation of neurotransmitters [55].

Tryptophan, found at higher concentrations in female mice in the three regions of the brain, is the precursor of 5-hydroxytryptophan (5-HTP) and serotonin (5-hydroxytryptamine, 5-HT), which are neurotransmitters regulating social behavior, aggressiveness and sexual arousal in male as well as female mice [56–59]. While 5-HT is consistently biosynthesized throughout the rat brain, males produce 52% more 5-HT than females, which may explain the higher concentration of tryptophan in female brains [60].

The oxidized form of methionine, sulfoxide methionine, is a biomarker of oxidative stress, which is physiologically reduced by methionine sulfoxide reductase. Methionine sulfoxide was detectable only in frontal cortices, with higher values in males compared to females, suggesting differences between male and female susceptibility to oxidative stress in the frontal cortex.

Tyrosine was found at higher concentrations in the frontal cortices and cerebellums of males, while both phenylalanine and dopamine were increased in female frontal cortices. Tyrosine, derived from phenylalanine, and its own derivatives, the catecholamine neurotransmitters L-DOPA, dopamine, norepinephrine and epinephrine play key roles in acute stress and arousal, focus and mood behaviors. Furthermore, higher tyrosine levels allow an increased turnover of catecholamines under stressful conditions, which may reflect a different response to stress [61].

Histamine is a nitrogenous compound that was found at a higher concentration in the frontal cortices and cerebellums of males than in females. It is involved in the inflammatory response

and acts as a neurotransmitter in the brain, modulating awareness and addictive behavior. Histamine also plays a role in motivation and addiction, particularly for food and alcohol, increasing satiety and decreasing food intake *via* H3 receptors. Histidine, the precursor of histamine, was also increased in the cerebellum of male mice, but not in the frontal cortex as in the case of histamine. Carnosine, a dipeptide composed of alanine and histidine, is a precursor of histidine [62]. Carnosine was increased in the cerebellum of males while histamine and histidine were increased in the brain stem. Peñafiel et al have already highlighted the up-regulation of carnosine by testosterone [63]. Carnosine is also known for its antioxidant effect in the brain in physiological concentrations in humans, at which its levels are higher than in the rest of the body [64].

The polyamine signature of sexual dimorphism

Polyamines (putrescine, spermine and spermidine) are organic compounds found in high concentrations in the brain. Males have higher levels of spermine and spermidine in the brain stem. Polyamines play pleiotropic roles in DNA maintenance, cell proliferation, differentiation, and longevity [65]. In the brain, they are stored in astrocytes [66], and have a neuromodulatory effect on almost all known receptors and channels, both at the intra- and extra-cellular levels [67]. Polyamines are especially prone to oxidative stress, and their oxidation can lead to the accumulation of toxic components such as aldehydes.

Integrating network and potential translational applications

A metabolomic signature artificially juxtaposes many structural and functional metabolite variations of different origins. **Fig. 7** aims at providing an integrative view of the main sexually induced variations that we globally observed in the brain. This network shows that some metabolites are at the crossroads of different metabolic pathways, connecting them to the others. Phospholipids, glycine, polyamines, proline, serotonin and dopamine illustrate these metabolic nodes creating the network. An unexpectedly sharp indirect impact of the systemic muscle and bone mass in the brain metabolome is also highlighted. At a higher level of integration, we have tried to connect this metabolic network to biological and physiological functions, highlighting the main consequences of the sexual variations of the metabolome. Interestingly, the influence of gender has already been noted in the brain for most of these biological functions, such as those observed in energetic metabolism [41,43], oxidative stress defenses [68], and neurotransmission and neuromodulation by the dopamine, serotonin and

GABAergic systems [69]. With regard to biological structures, the network shows that myelin and cell membrane composition are also highly impacted by sex.

The final level of integration concerns potential translational consequences that could be inferred from such a network. Most neurodevelopmental, neurodegenerative and neuropsychiatric disorders are influenced by sex in terms of prevalence, severity of clinical expression and response to treatments. For example, in female mice we found an increase of sphingomyelins, known to compose the myelin sheath, whereas in male mice we found an increase of lysophosphatidylcholines, known to induce myelin sheath degradation. This is consistent with studies showing an increased turnover of oligodendrocytes and myelin sheath in male rodents due to long-term effects of androgen [70]. We may speculate that such sex differences in the composition of the myelin sheath may explain, in cases of multiple sclerosis, either the higher prevalence in women or the less severe prognostic in women despite their stronger immune response than in men [71]. Concerning Parkinson's disease, a number of gender differences have been documented in clinical expression such as a lesser severity and a later onset in women compared to men [72]. The increased dopamine levels that we observed in frontal cortices may contribute to these variations of clinical expression. Prefrontal cortex dopamine levels are also known to strongly influence depression [73], a disorder known to be highly influenced by sex [74]. The therapeutic, sex-based disparity in response to diverse treatments has also been observed in neurons in culture, in the mouse brain and in human neurological disease [75]. It is likely that the metabolic dimorphism observed here plays a role in the variation of response to treatment, particularly affecting the processes of neurotransmission and neuromodulation. These examples show that the metabolic mapping of cerebral regions could be particularly useful for understanding how sex contributes to differences in phenotypic expression, and to better stratify the treatments according to the sex differences.

Limits

This pilot study focused only on limited subsets of the brain metabolome and regions, and needs to be extended to provide a complete overview of the sexual dimorphism of the brain.

Conclusion

In total, the metabolites involved in the sexual dimorphism play key roles in a wide range of both systemic and local brain functions: richness in collagen (hydroxyproline, proline, creatinine) of the whole body, energetic metabolism (hexoses, acylcarnitines, and creatinine), neurotransmission and neuromodulation (phosphatidylcholines, proline, glycine, serine, threonine, lysine, tryptophan, tyrosine, histamine, histidine, carnosine, and polyamines), membrane structure and cell composition (phosphatidylcholines, lysophosphatidylcholines, and sphingomyelins), myelin metabolism (lysophosphatidylcholines and sphingomyelins), oxidative stress (methionine, sulfoxide methionine, carnosine, and polyamines), folate metabolism (serine, and methionine), and finally, the cell signaling system (polyamines).

In conclusion, the metabolic sexual dimorphism is major in the brain, affecting half the sampling of the metabolites measured here, with wide regional variations and involving a large number of structures and functions. The fine mapping of this metabolic dimorphism will be useful in the coming years, both to better integrate the physiological differences between the sexes, but also to better understand how and why the clinical expression of the neurological diseases is influenced by gender.

Figure legends

Fig. 1. **Overall study design divided into two workflows. (A)**, the analytical pipeline, which describes the collection and pre-processing of data; and **(B),** the statistical pipeline, which describes the analytical steps applied to each dataset obtained.

Fig. 2. **Unsupervised analysis of the whole dataset.** The first plan **(A, C)** and the second plan **(B, D)** of the PCA are shown. Colors according to tissue **(A, B)** or gender **(C, D)**.

Fig. 3. Relative distribution of metabolites in the brain regions studied. The positions of the compounds are determined according to mean concentrations in the brain stem, the frontal cortex and the cerebellum. Label sizes are set according to the VIP, the compounds with larger labels having a higher VIP.

Fig. 4. Sex dimorphic metabolites for the whole dataset. (A): Volcano plot of OPLS-DA results. Compounds at the top of the plot are the most important for gender discrimination. Left-most compounds have higher values in females, while right-most compounds have higher values in males. **(B):** Word cloud computed using metabolite VIPs to determine the size of the labels, and loadings to determine the color scale, from deep blue for high negative loadings (increased in females) to deep red for high positive loadings (increased in males).

Fig. 5. **Sex dimorphic metabolites in individual tissues.** Volcano plots and their corresponding word clouds for brain stem **(A, B)**, frontal cortex **(C, D)** and cerebellum **(E, F)**. Metabolites on the volcano plots are positioned according to their VIP (y-axis) and loadings (x-axis). Word clouds were computed using metabolite VIPs to determine the size of the labels, and loadings to determine the color scale, from deep blue for high negative loadings (increased in females) to deep red for high positive loadings (increased in males).

Fig. 6. **Metabolome tissue-specific and non-tissue-specific sex dimorphism.** Venn diagram showing metabolites with a sexual dimorphism in either brain stem, frontal cortex or cerebellum separately, or shared between two or three of these three tissues. Colored backgrounds under the metabolites indicate whether they are increased in females (blue) or males (red). Metabolites marked with an asterisk (*) have a different direction of variation in each tissue.

Fig. 7. Functional projection of the metabolomic sex dimorphism observed in the mouse brain. Metabolites are pictured as yellow nodes, while biological pathways linked to these metabolites are pictured as green nodes. Red-labeled metabolites showed sexual dimorphism

in at least one of the three brain regions studied, while black-labeled metabolites did not show any quantitative sexual dimorphism. Gray-labeled metabolites were not analyzed in this study. Node sizes were determined according to the number of other nodes linked.

Acknowledgments:

We are grateful to Kanaya Malkani for critical reading and comments on the manuscript and to the team of the *Service Commun d'Animalerie Hospitalo-Universitaire* (SCAHU) of the University of Angers for animal facilities.

Funding:

This study was supported by the *Institut National de la Santé et de la Recherche Médicale* (*INSERM)*, the *Centre National de la Recherche Scientifique* (*CNRS)*, the *University of Angers*, and the *University Hospital of Angers*.

Competing interests:

None declared.

Supplementary Materials:

Supplementary Fig. 1. Supervised models' scores for samples after tissue and sex classification, on the whole dataset. **(A):** Tissue discrimination using PLS-DA ($Q2_C$ = 0.965). Frontal cortex samples are colored in green, cerebellum samples in red and brain stem samples in blue. **(B):** Gender discrimination using OPLS-DA ($Q2_C$ = 0.816). Females are plotted in blue while males are plotted in red.

Supplementary Fig. 2. Supervised models' scores for samples after sex classification in individual tissues. Gender discrimination using OPLS-DA for brain stem **(A)**, frontal cortex **(B)** and Cerebellum **(C)**. Males are plotted in red, while females are plotted in blue. $Q2_C$ are 0.837, 0.557 and 0.467 for brain stem, frontal cortex and cerebellum, respectively.

Supplementary Table 1. Raw data.

Supplementary Table 2. Whole dataset unsupervised analysis results.

Supplementary Table 3. Whole dataset supervised analysis results.

References and Notes:

[1] Zucker I, Beery AK. Males still dominate animal studies. Nature 2010;465:690. doi:10.1038/465690a.

[2] Yoon DY, Mansukhani NA, Stubbs VC, Helenowski IB, Woodruff TK, Kibbe MR. Sex bias exists in basic science and translational surgical research. Surgery 2014;156:508–16. doi:10.1016/j.surg.2014.07.001.

[3] Franconi F, Brunelleschi S, Steardo L, Cuomo V. Gender differences in drug responses. Pharmacol Res 2007;55:81–95. doi:10.1016/j.phrs.2006.11.001.

[4] U. S. Government Accountability Office. Drug Safety: Most Drugs Withdrawn in Recent Years Had Greater Health Risks for Women 2001.

[5] Sandberg K, Umans JG, Georgetown Consensus Conference Work Group. Recommendations concerning the new U.S. National Institutes of Health initiative to balance the sex of cells and animals in preclinical research. FASEB J 2015;29:1646–52. doi:10.1096/fj.14-269548.

[6] Clayton JA, Collins FS. Policy: NIH to balance sex in cell and animal studies. Nature 2014;509:282–3.

[7] Dayton A, Exner EC, Bukowy JD, Stodola TJ, Kurth T, Skelton M, et al. Breaking the Cycle: Estrous Variation Does Not Require Increased Sample Size in the Study of Female Rats. Hypertension 2016;68:1139–44. doi:10.1161/HYPERTENSIONAHA.116.08207.

[8] Hoffman JM, Soltow QA, Li S, Sidik A, Jones DP, Promislow DEL. Effects of age, sex, and genotype on high-sensitivity metabolomic profiles in the fruit fly, Drosophila melanogaster. Aging Cell 2014;13:596–604. doi:10.1111/acel.12215.

[9] Bovo S, Mazzoni G, Calò DG, Galimberti G, Fanelli F, Mezzullo M, et al. Deconstructing the pig sex metabolome: Targeted metabolomics in heavy pigs revealed sexual dimorphisms in plasma biomarkers and metabolic pathways. J Anim Sci 2015;93:5681–93. doi:10.2527/jas.2015-9528.

[10] Liang Q, Xu W, Hong Q, Xiao C, Yang L, Ma Z, et al. Rapid comparison of metabolites in humans and rats of different sexes using untargeted UPLC-TOFMS and an in-house software platform. Eur J Mass Spectrom (Chichester) 2015;21:801–21. doi:10.1255/ejms.1395.

[11] Saito K, Maekawa K, Kinchen JM, Tanaka R, Kumagai Y, Saito Y. Gender- and Age-Associated Differences in Serum Metabolite Profiles among Japanese Populations. Biol Pharm Bull 2016;39:1179–86. doi:10.1248/bpb.b16-00226.

[12] Audano M, Maldini M, De Fabiani E, Mitro N, Caruso D. Gender-related metabolomics and lipidomics: From experimental animal models to clinical evidence. Journal of Proteomics 2018;178:82–91. doi:10.1016/j.jprot.2017.11.001.

[13] Mittelstrass K, Ried JS, Yu Z, Krumsiek J, Gieger C, Prehn C, et al. Discovery of sexual dimorphisms in metabolic and genetic biomarkers. PLoS Genet 2011;7:e1002215. doi:10.1371/journal.pgen.1002215.

[14] Decsi T, Kennedy K. Sex-specific differences in essential fatty acid metabolism. The American Journal of Clinical Nutrition 2011;94:1914S-1919S. doi:10.3945/ajcn.110.000893.

[15] Childs CE, Romeu-Nadal M, Burdge GC, Calder PC. The Polyunsaturated Fatty Acid Composition of Hepatic and Plasma Lipids Differ by Both Sex and Dietary Fat Intake in Rats. The Journal of Nutrition 2010;140:245–50. doi:10.3945/jn.109.115691.
[16] Brunelli E, Domanico F, La Russa D, Pellegrino D. Sex differences in oxidative stress biomarkers. Curr Drug Targets 2014;15:811–5.
[17] Chao de la Barca JM, Simard G, Sarzi E, Chaumette T, Rousseau G, Chupin S, et al. Targeted Metabolomics Reveals Early Dominant Optic Atrophy Signature in Optic Nerves of *Opa1* $^{delTTAG/+}$ Mice. Investigative Opthalmology & Visual Science 2017;58:812. doi:10.1167/iovs.16-21116.
[18] Sarzi E, Seveno M, Angebault C, Milea D, Rönnbäck C, Quilès M, et al. Increased steroidogenesis promotes early-onset and severe vision loss in females with *OPA1* dominant optic atrophy. Human Molecular Genetics 2016:ddw117. doi:10.1093/hmg/ddw117.
[19] Spring S, Lerch JP, Henkelman RM. Sexual dimorphism revealed in the structure of the mouse brain using three-dimensional magnetic resonance imaging. Neuroimage 2007;35:1424–33. doi:10.1016/j.neuroimage.2007.02.023.
[20] Raznahan A, Probst F, Palmert MR, Giedd JN, Lerch JP. High resolution whole brain imaging of anatomical variation in XO, XX, and XY mice. Neuroimage 2013;83:962–8. doi:10.1016/j.neuroimage.2013.07.052.
[21] Goldstein JM, Seidman LJ, Horton NJ, Makris N, Kennedy DN, Caviness VS, et al. Normal sexual dimorphism of the adult human brain assessed by in vivo magnetic resonance imaging. Cereb Cortex 2001;11:490–7.
[22] Nopoulos P, Flaum M, O'Leary D, Andreasen NC. Sexual dimorphism in the human brain: evaluation of tissue volume, tissue composition and surface anatomy using magnetic resonance imaging. Psychiatry Res 2000;98:1–13.
[23] Joel D, Berman Z, Tavor I, Wexler N, Gaber O, Stein Y, et al. Sex beyond the genitalia: The human brain mosaic. Proceedings of the National Academy of Sciences 2015;112:15468–73. doi:10.1073/pnas.1509654112.
[24] Chung WCJ, Auger AP. Gender differences in neurodevelopment and epigenetics. Pflügers Archiv - European Journal of Physiology 2013;465:573–84. doi:10.1007/s00424-013-1258-4.
[25] Trabzuni D, Ramasamy A, Imran S, Walker R, Smith C, Weale ME, et al. Widespread sex differences in gene expression and splicing in the adult human brain. Nat Commun 2013;4:2771. doi:10.1038/ncomms3771.
[26] Tsai I-L, Kuo T-C, Ho T-J, Harn Y-C, Wang S-Y, Fu W-M, et al. Metabolomic Dynamic Analysis of Hypoxia in MDA-MB-231 and the Comparison with Inferred Metabolites from Transcriptomics Data. Cancers (Basel) 2013;5:491–510. doi:10.3390/cancers5020491.
[27] Yang X. Tissue-specific expression and regulation of sexually dimorphic genes in mice. Genome Research 2006;16:995–1004. doi:10.1101/gr.5217506.
[28] Overmyer KA, Thonusin C, Qi NR, Burant CF, Evans CR. Impact of Anesthesia and Euthanasia on Metabolomics of Mammalian Tissues: Studies in a C57BL/6J Mouse Model. PLoS One 2015;10. doi:10.1371/journal.pone.0117232.

[29] Zukunft S, Prehn C, Röhring C, Möller G, Hrabě de Angelis M, Adamski J, et al. High-throughput extraction and quantification method for targeted metabolomics in murine tissues. Metabolomics 2018;14. doi:10.1007/s11306-017-1312-x.
[30] Chao de la Barca JM, Simard G, Amati-Bonneau P, Safiedeen Z, Prunier-Mirebeau D, Chupin S, et al. The metabolomic signature of Leber's hereditary optic neuropathy reveals endoplasmic reticulum stress. Brain 2016;139:2864–76. doi:10.1093/brain/aww222.
[31] Worley B, Powers R. Multivariate Analysis in Metabolomics. Current Metabolomics 2013;1:92. doi:10.2174/2213235X11301010092.
[32] Galindo-Prieto B, Eriksson L, Trygg J. Variable influence on projection (VIP) for orthogonal projections to latent structures (OPLS). Journal of Chemometrics 2014;28:623–32. doi:10.1002/cem.2627.
[33] R Development Core Team. R: A language and environment for statistical computing. R Foundation for Statistical Computing, Vienna, Austria: 2008.
[34] FactoMineR: An R Package for Multivariate Analysis | Lê | Journal of Statistical Software. Journal of Statistical Software 2008;25. doi:10.18637/jss.v025.i01.
[35] Thévenot EA, Roux A, Xu Y, Ezan E, Junot C. Analysis of the Human Adult Urinary Metabolome Variations with Age, Body Mass Index, and Gender by Implementing a Comprehensive Workflow for Univariate and OPLS Statistical Analyses. Journal of Proteome Research 2015;14:3322–35. doi:10.1021/acs.jproteome.5b00354.
[36] Jaeger C, Glaab E, Michelucci A, Binz TM, Koeglsberger S, Garcia P, et al. The mouse brain metabolome: region-specific signatures and response to excitotoxic neuronal injury. Am J Pathol 2015;185:1699–712. doi:10.1016/j.ajpath.2015.02.016.
[37] O'Brien JS, Sampson EL. Lipid composition of the normal human brain: gray matter, white matter, and myelin. J Lipid Res 1965;6:537–44.
[38] Zeisel SH. Metabolic crosstalk between choline/1-carbon metabolism and energy homeostasis. Clinical Chemistry and Laboratory Medicine 2012;51:467–475. doi:10.1515/cclm-2012-0518.
[39] Trabado S, Al-Salameh A, Croixmarie V, Masson P, Corruble E, Fève B, et al. The human plasma-metabolome: Reference values in 800 French healthy volunteers; impact of cholesterol, gender and age. PLOS ONE 2017;12:e0173615. doi:10.1371/journal.pone.0173615.
[40] Ousman SS, David S. Lysophosphatidylcholine induces rapid recruitment and activation of macrophages in the adult mouse spinal cord. Glia 2000;30:92–104. doi:10.1002/(SICI)1098-1136(200003)30:1<92::AID-GLIA10>3.0.CO;2-W.
[41] Nagai K, Yoshida S, Konishi H. Gender differences in the gene expression profiles of glucose transporter GLUT class I and SGLT in mouse tissues. Pharmazie 2014;69:856–9.
[42] Gaignard P, Fréchou M, Liere P, Thérond P, Schumacher M, Slama A, et al. Sex differences in brain mitochondrial metabolism: influence of endogenous steroids and stroke. Journal of Neuroendocrinology 2018;30:e12497. doi:10.1111/jne.12497.
[43] Yoshizawa H, Gazes Y, Stern Y, Miyata Y, Uchiyama S. Characterizing the normative profile of 18F-FDG PET brain imaging: Sex difference, aging effect, and cognitive

reserve. Psychiatry Research: Neuroimaging 2014;221:78–85. doi:10.1016/j.pscychresns.2013.10.009.
[44] Ruoppolo M, Caterino M, Albano L, Pecce R, Di Girolamo MG, Crisci D, et al. Targeted metabolomic profiling in rat tissues reveals sex differences. Scientific Reports 2018;8:4663. doi:10.1038/s41598-018-22869-7.
[45] Borum PR. Variation in tissue carnitine concentrations with age and sex in the rat. Biochem J 1978;176:677–81.
[46] Nieves JW, Formica C, Ruffing J, Zion M, Garrett P, Lindsay R, et al. Males have larger skeletal size and bone mass than females, despite comparable body size. J Bone Miner Res 2005;20:529–35. doi:10.1359/JBMR.041005.
[47] Mauvais-Jarvis F. Sex differences in metabolic homeostasis, diabetes, and obesity. Biol Sex Differ 2015;6. doi:10.1186/s13293-015-0033-y.
[48] Montes GS, Bezerra MSF, Junqueira LCU. Collagen distribution in tissues. Ultrastructure of the Connective Tissue Matrix, Springer, Boston, MA; 1984, p. 65–88. doi:10.1007/978-1-4613-2831-5_3.
[49] Ortiz JG, Negrón AE, Bruno MS. High-affinity binding of proline to mouse brain synaptic membranes. Neurochem Res 1989;14:139–42. doi:10.1007/BF00969628.
[50] Wyse ATS, Netto CA. Behavioral and neurochemical effects of proline. Metab Brain Dis 2011;26:159. doi:10.1007/s11011-011-9246-x.
[51] Legendre P. The glycinergic inhibitory synapse. Cell Mol Life Sci 2001;58:760–93.
[52] Boehm G, Cervantes H, Georgi G, Jelinek J, Sawatzki G, Wermuth B, et al. Effect of Increasing Dietary Threonine Intakes on Amino Acid Metabolism of the Central Nervous System and Peripheral Tissues in Growing Rats. Pediatric Research 1998;44:900–6. doi:10.1203/00006450-199812000-00013.
[53] Kasé Y, Kataoka M, Miyata T, Okano Y. Pipecolic acid in the dog brain. Life Sciences 1973;13:867–73. doi:10.1016/0024-3205(73)90077-5.
[54] Nishio H, Segawa T. Determination of pipecolic acid in rat brain areas by high-performance liquid chromatography of dansyl derivatives with fluorimetric detection. Analytical Biochemistry 1983;135:312–7. doi:10.1016/0003-2697(83)90688-7.
[55] Hallen A, Jamie JF, Cooper AJL. Lysine metabolism in mammalian brain: an update on the importance of recent discoveries. Amino Acids 2013;45. doi:10.1007/s00726-013-1590-1.
[56] Zhang WQ, Smolik CM, Barba-Escobedo PA, Gamez M, Sanchez JJ, Javors MA, et al. Acute Dietary Tryptophan Manipulation Differentially Alters Social Behavior, Brain Serotonin and Plasma Corticosterone in Three Inbred Mouse Strains. Neuropharmacology 2015;90:1–8. doi:10.1016/j.neuropharm.2014.10.024.
[57] Kulikov AV, Osipova DV, Naumenko VS, Terenina E, Mormède P, Popova NK. A pharmacological evidence of positive association between mouse intermale aggression and brain serotonin metabolism. Behavioural Brain Research 2012;233:113–9. doi:10.1016/j.bbr.2012.04.031.
[58] Liu Y, Jiang Y, Si Y, Kim J-Y, Chen Z-F, Rao Y. Molecular Regulation of Sexual Preference Revealed by Genetic Studies of 5-HT in the Brain of Male Mice. Nature 2011;472:95–9. doi:10.1038/nature09822.

[59] Zhang S, Liu Y, Rao Y. Serotonin signaling in the brain of adult female mice is required for sexual preference. Proc Natl Acad Sci U S A 2013;110:9968–73. doi:10.1073/pnas.1220712110.
[60] Nishizawa S, Benkelfat C, Young SN, Leyton M, Mzengeza S, de Montigny C, et al. Differences between males and females in rates of serotonin synthesis in human brain. Proc Natl Acad Sci U S A 1997;94:5308–13.
[61] Lieberman HR. Tyrosine and Stress: Human and Animal Studies. National Academies Press (US); 1994.
[62] Bae O-N, Majid A. Role of histidine/histamine in carnosine-induced neuroprotection during ischemic brain damage. Brain Research 2013;1527:246–54. doi:10.1016/j.brainres.2013.07.004.
[63] Peñafiel R, Ruzafa C, Monserrat F, Cremades A. Gender-related differences in carnosine, anserine and lysine content of murine skeletal muscle. Amino Acids 2004;26:53–8. doi:10.1007/s00726-003-0034-8.
[64] Mendelson SD. 10 - NUTRITIONAL SUPPLEMENTS AND METABOLIC SYNDROME. In: Mendelson SD, editor. Metabolic Syndrome and Psychiatric Illness, San Diego: Academic Press; 2008, p. 141–86. doi:10.1016/B978-012374240-7.50012-7.
[65] Lenis YY, Elmetwally MA, Maldonado-Estrada JG, Bazer FW. Physiological importance of polyamines. Zygote 2017;25:244–55. doi:10.1017/S0967199417000120.
[66] Benedikt J, Inyushin M, Kucheryavykh YV, Rivera Y, Kucheryavykh LY, Nichols CG, et al. Intracellular Polyamines Enhance Astrocytic Coupling. Neuroreport 2012;23:1021–5. doi:10.1097/WNR.0b013e32835aa04b.
[67] Skatchkov S, Woodbury M, Eaton M. The Role of Glia in Stress: Polyamines and Brain Disorders. Psychiatr Clin North Am 2014;37:653–78. doi:10.1016/j.psc.2014.08.008.
[68] Ruszkiewicz JA, Miranda-Vizuete A, Tinkov AA, Skalnaya MG, Skalny AV, Tsatsakis A, et al. Sex-Specific Differences in Redox Homeostasis in Brain Norm and Disease. J Mol Neurosci 2019;67:312–42. doi:10.1007/s12031-018-1241-9.
[69] Rezzani R, Franco C, Rodella LF. Sex differences of brain and their implications for personalized therapy. Pharmacol Res 2019;141:429–42. doi:10.1016/j.phrs.2019.01.030.
[70] Ghanem CA, Degerny C, Hussain R, Liere P, Pianos A, Tourpin S, et al. Long-lasting masculinizing effects of postnatal androgens on myelin governed by the brain androgen receptor. PLOS Genetics 2017;13:e1007049. doi:10.1371/journal.pgen.1007049.
[71] Voskuhl RR, Gold SM. Sex-related factors in multiple sclerosis susceptibility and progression. Nature Reviews Neurology 2012;8:255–63. doi:10.1038/nrneurol.2012.43.
[72] Miller IN, Cronin-Golomb A. GENDER DIFFERENCES IN PARKINSON'S DISEASE: CLINICAL CHARACTERISTICS AND COGNITION. Mov Disord 2010;25:2695–703. doi:10.1002/mds.23388.
[73] Vialou V. Dépression et régulation de l'activité dopaminergique. Med Sci (Paris) 2013;29:473–7. doi:10.1051/medsci/2013295010.
[74] Albert PR. Why is depression more prevalent in women? J Psychiatry Neurosci 2015;40:219–21. doi:10.1503/jpn.150205.
[75] Manole MD, Tehranian-DePasquale R, Du L, Bayır H, Clark PMK and RSB. Unmasking Sex-Based Disparity in Neuronal Metabolism. Current Pharmaceutical Design 2011. http://www.eurekaselect.com/75806/article.

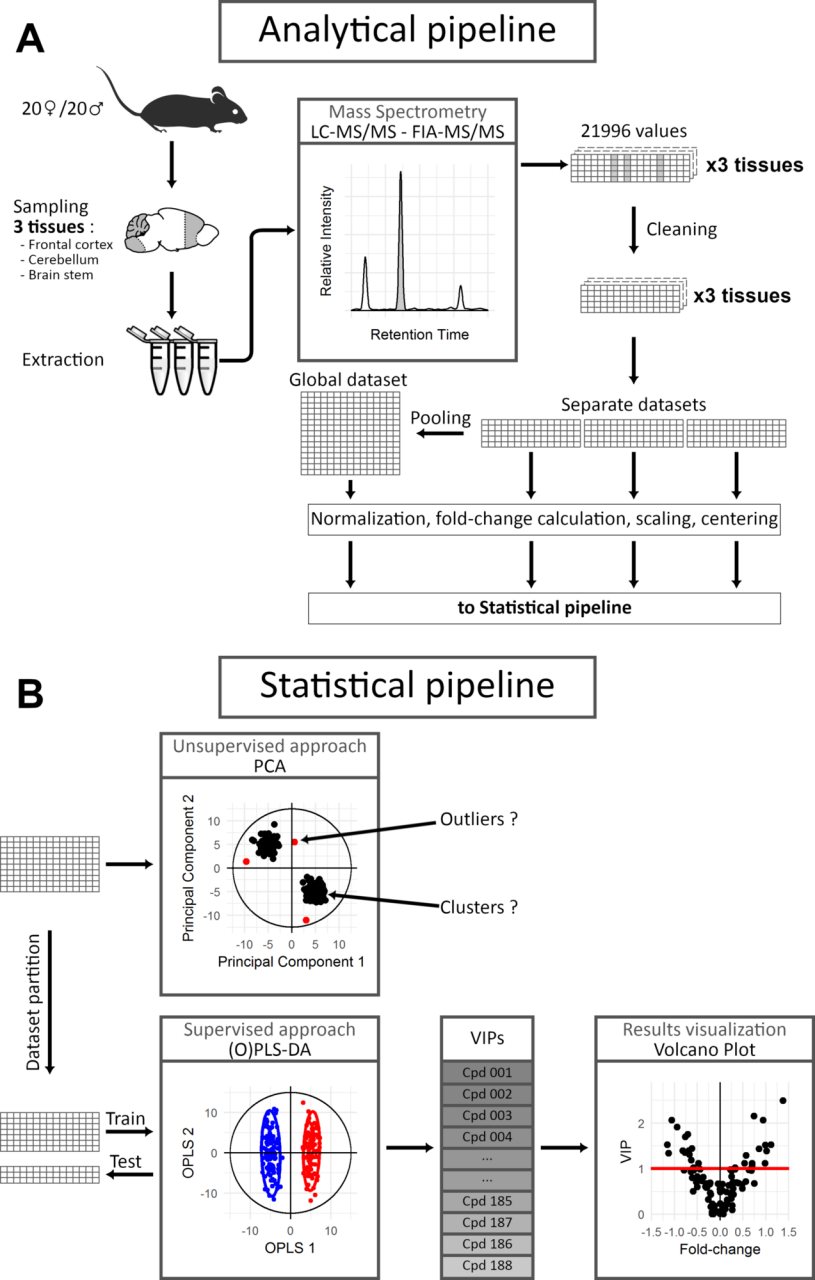
A
Analytical pipeline
20♀/20♂
Sampling
3 tissues :
- Frontal cortex
- Cerebellum
- Brain stem
Extraction
Mass Spectrometry
LC-MS/MS - FIA-MS/MS
Relative Intensity
Retention Time
21996 values
x3 tissues
Cleaning
x3 tissues
Global dataset
Pooling
Separate datasets
Normalization, fold-change calculation, scaling, centering
to Statistical pipeline
B
Statistical pipeline
Unsupervised approach
PCA
Principal Component 2
Principal Component 1
Outliers ?
Clusters ?
Dataset partition
Train
Test
Supervised approach
(O)PLS-DA
OPLS 2
OPLS 1
VIPs
Cpd 001
Cpd 002
Cpd 003
Cpd 004
...
...
Cpd 185
Cpd 187
Cpd 186
Cpd 188
Results visualization
Volcano Plot
VIP
Fold-change

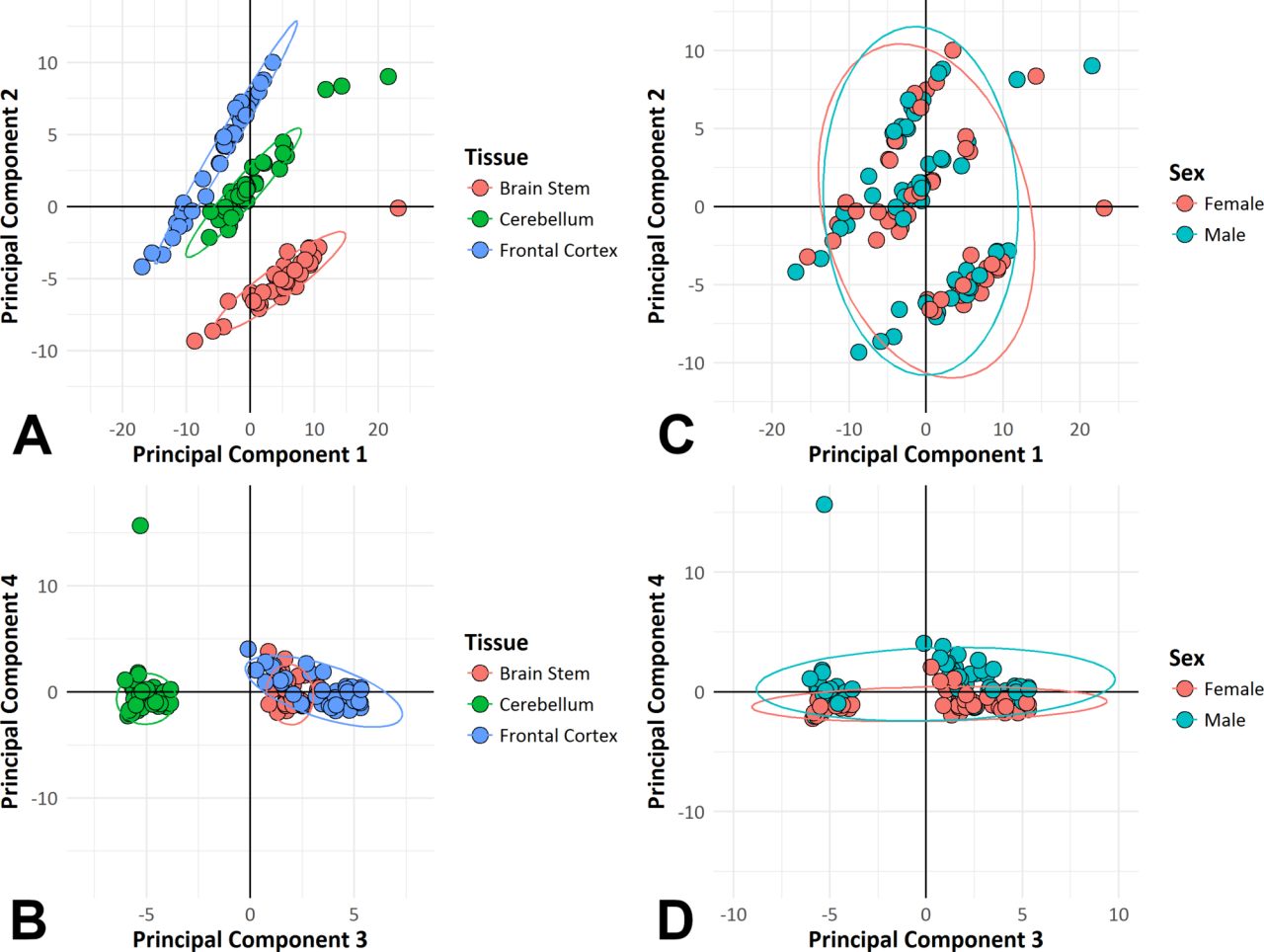
A
Principal Component 2
Principal Component 1
10
5
0
-5
-10
-20
-10
0
10
20
Tissue
Brain Stem
Cerebellum
Frontal Cortex
B
Principal Component 4
Principal Component 3
10
0
-10
-5
0
5
Tissue
Brain Stem
Cerebellum
Frontal Cortex
C
Principal Component 2
Principal Component 1
10
5
0
-5
-10
-20
-10
0
10
20
Sex
Female
Male
D
Principal Component 4
Principal Component 3
10
0
-10
-10
-5
0
5
10
Sex
Female
Male

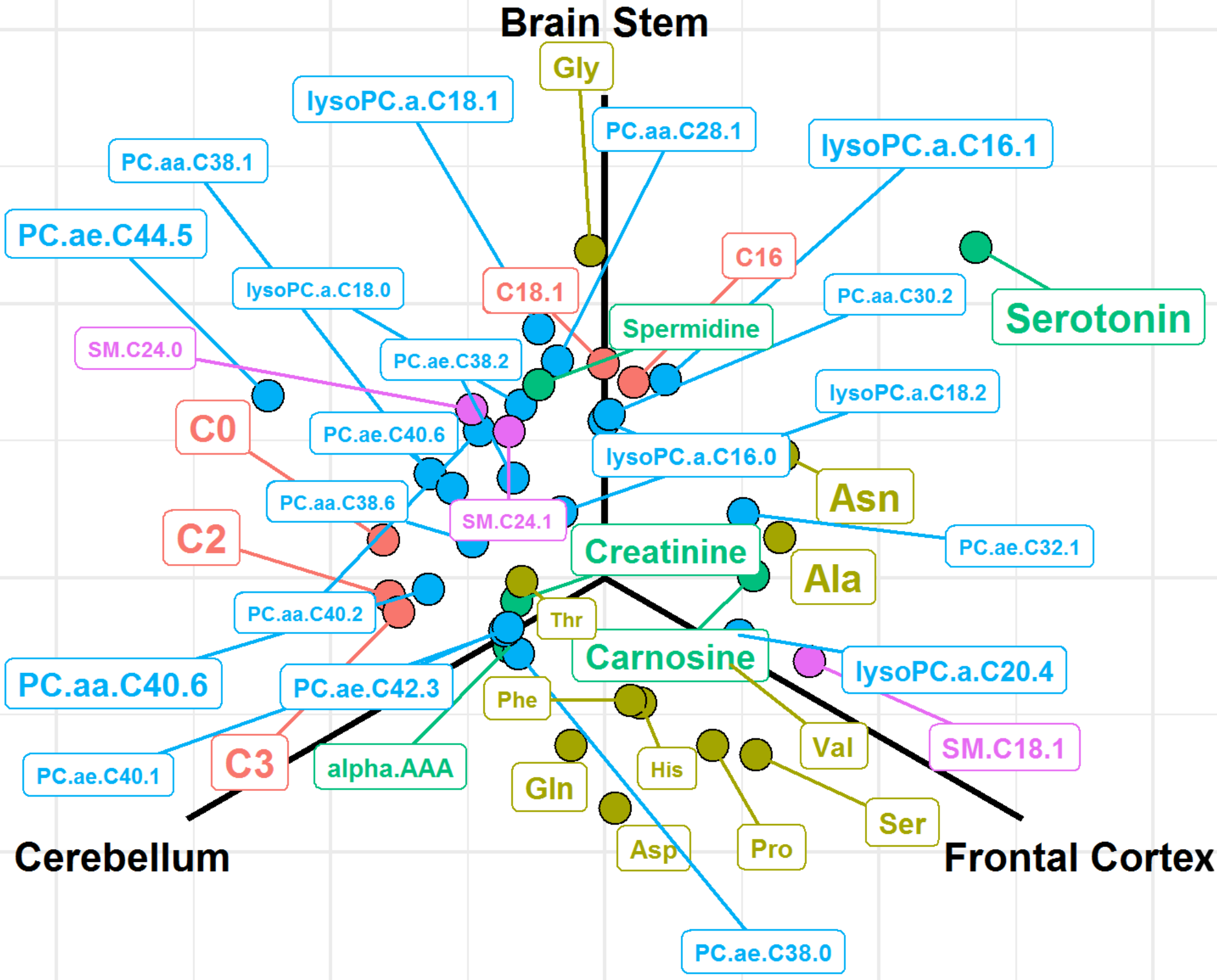
Brain Stem
Gly
lysoPC.a.C18.1
PC.aa.C28.1
lysoPC.a.C16.1
PC.aa.C38.1
PC.ae.C44.5
C16
Serotonin
lysoPC.a.C18.0
C18.1
PC.aa.C30.2
Spermidine
SM.C24.0
PC.ae.C38.2
lysoPC.a.C18.2
C0
PC.ae.C40.6
lysoPC.a.C16.0
Asn
PC.aa.C38.6
SM.C24.1
C2
Creatinine
PC.ae.C32.1
Ala
PC.aa.C40.2
Thr
Carnosine
lysoPC.a.C20.4
PC.aa.C40.6
PC.ae.C42.3
Phe
Val
SM.C18.1
PC.ae.C40.1
C3
alpha.AAA
His
Gln
Ser
Asp
Pro
Cerebellum
Frontal Cortex
PC.ae.C38.0

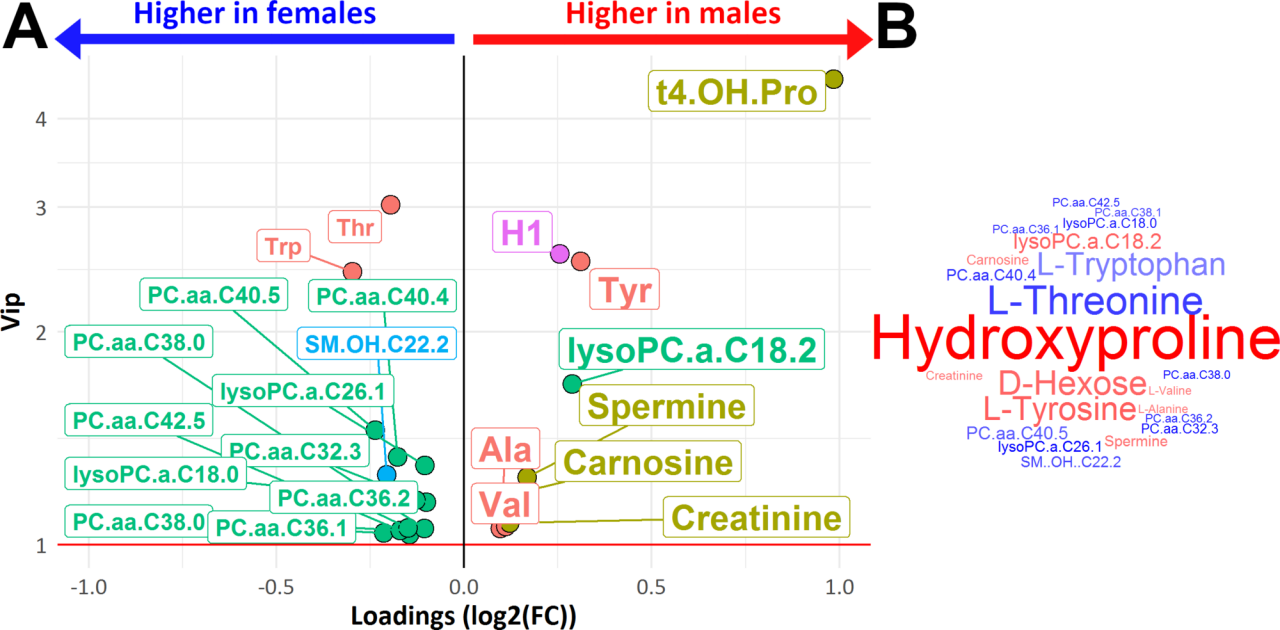
A
Higher in females
Higher in males
B
t4.OH.Pro
H1
Tyr
Thr
Trp
PC.aa.C40.5
PC.aa.C40.4
SM.OH.C22.2
PC.aa.C38.0
lysoPC.a.C18.2
lysoPC.a.C26.1
Spermine
PC.aa.C42.5
PC.aa.C32.3
Ala
Carnosine
lysoPC.a.C18.0
PC.aa.C36.2
Val
PC.aa.C38.0
PC.aa.C36.1
Creatinine
Vip
4
3
2
1
-1.0
-0.5
0.0
0.5
1.0
Loadings (log2(FC))
PC.aa.C42.5
PC.aa.C38.1
lysoPC.a.C18.0
PC.aa.C36.1
lysoPC.a.C18.2
Carnosine
L-Tryptophan
PC.aa.C40.4
L-Threonine
Hydroxyproline
Creatinine
D-Hexose
PC.aa.C38.0
L-Valine
L-Tyrosine
L-Alanine
PC.aa.C36.2
PC.aa.C40.5
PC.aa.C32.3
Spermine
lysoPC.a.C26.1
SM..OH..C22.2

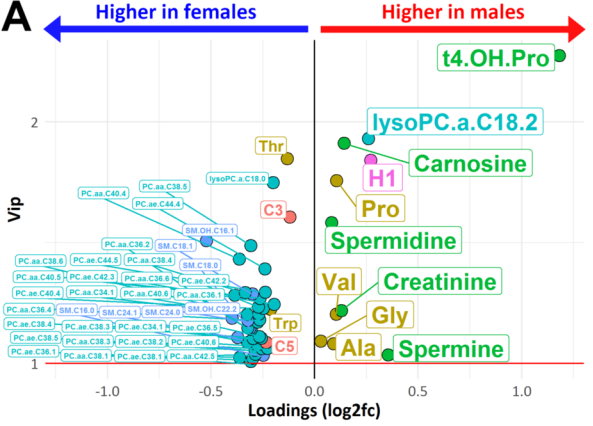
A
Higher in females
Higher in males
t4.OH.Pro
lysoPC.a.C18.2
Carnosine
H1
Pro
Spermidine
Val
Creatinine
Gly
Ala
Spermine
Thr
C3
C5
Trp
Vip
Loadings (log2fc)

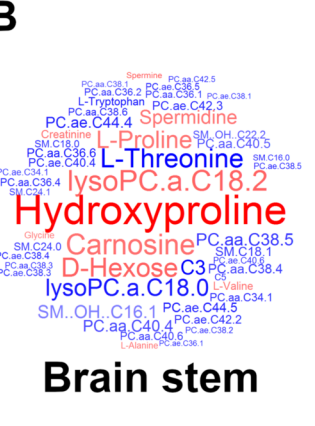
B
Brain stem

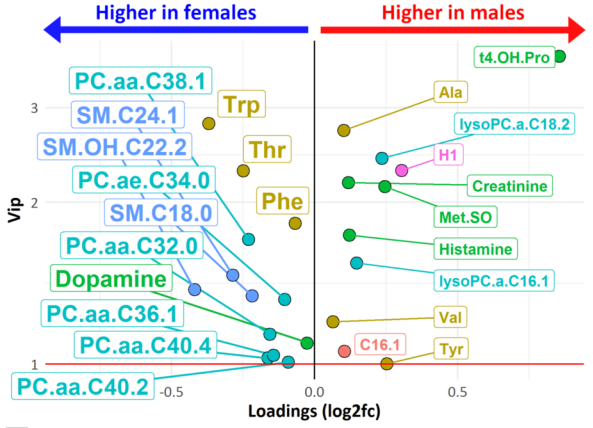
Higher in females
Higher in males
t4.OH.Pro
PC.aa.C38.1
SM.C24.1
SM.OH.C22.2
PC.ae.C34.0
SM.C18.0
PC.aa.C32.0
Dopamine
PC.aa.C36.1
PC.aa.C40.4
PC.aa.C40.2
Trp
Thr
Phe
Ala
lysoPC.a.C18.2
H1
Creatinine
Met.SO
Histamine
lysoPC.a.C16.1
Val
C16.1
Tyr
Vip
Loadings (log2fc)

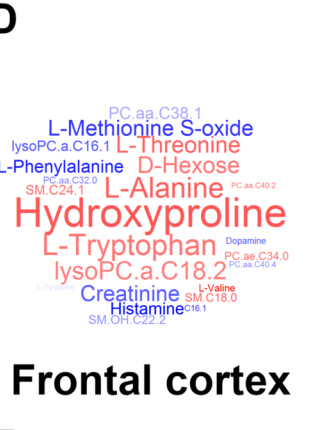
D
Frontal cortex

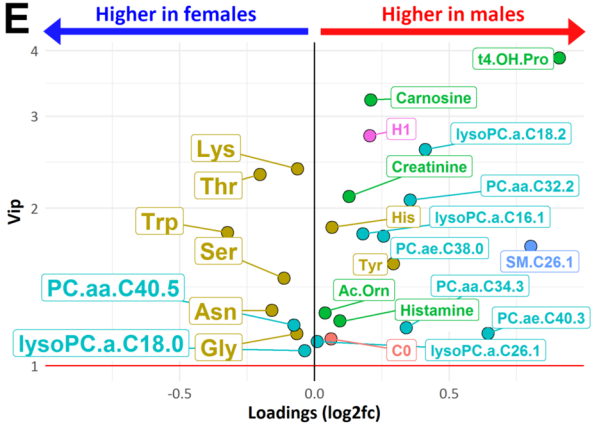
E
Higher in females
Higher in males
t4.OH.Pro
Carnosine
H1
lysoPC.a.C18.2
Creatinine
PC.aa.C32.2
His
lysoPC.a.C16.1
PC.ae.C38.0
Tyr
SM.C26.1
Ac.Orn
PC.aa.C34.3
Histamine
PC.ae.C40.3
C0
lysoPC.a.C26.1
Lys
Thr
Trp
Ser
PC.aa.C40.5
Asn
lysoPC.a.C18.0
Gly
Vip
Loadings (log2fc)

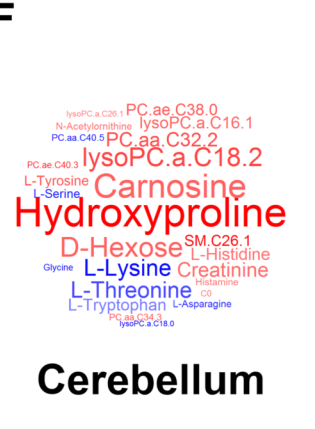
F
Cerebellum

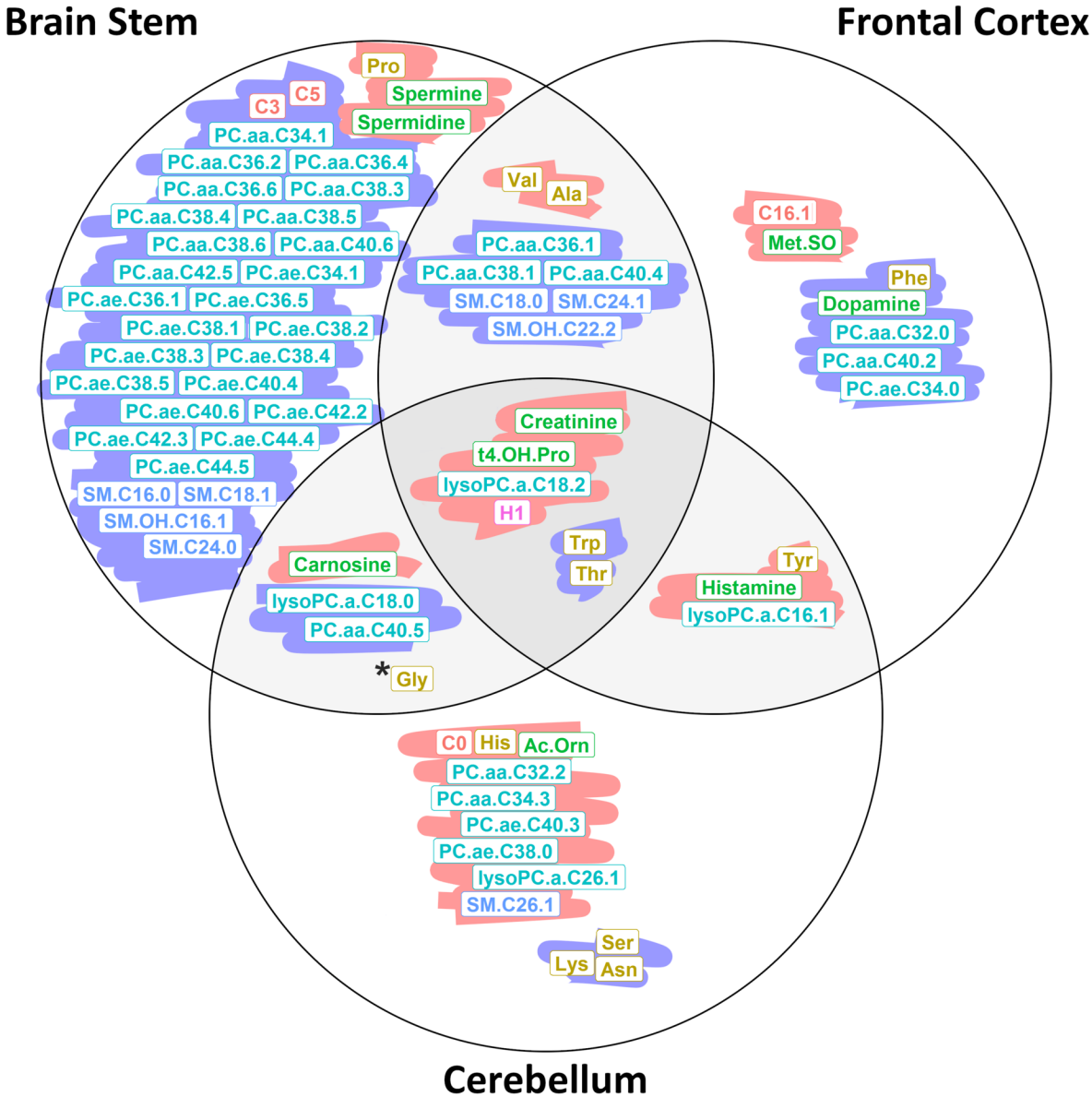
Brain Stem
Frontal Cortex
Cerebellum
Pro
Spermine
Spermidine
C5
C3
PC.aa.C34.1
PC.aa.C36.2
PC.aa.C36.4
PC.aa.C36.6
PC.aa.C38.3
PC.aa.C38.4
PC.aa.C38.5
PC.aa.C38.6
PC.aa.C40.6
PC.aa.C42.5
PC.ae.C34.1
PC.ae.C36.1
PC.ae.C36.5
PC.ae.C38.1
PC.ae.C38.2
PC.ae.C38.3
PC.ae.C38.4
PC.ae.C38.5
PC.ae.C40.4
PC.ae.C40.6
PC.ae.C42.2
PC.ae.C42.3
PC.ae.C44.4
PC.ae.C44.5
SM.C16.0
SM.C18.1
SM.OH.C16.1
SM.C24.0
Val
Ala
PC.aa.C36.1
PC.aa.C38.1
PC.aa.C40.4
SM.C18.0
SM.C24.1
SM.OH.C22.2
C16.1
Met.SO
Phe
Dopamine
PC.aa.C32.0
PC.aa.C40.2
PC.ae.C34.0
Creatinine
t4.OH.Pro
lysoPC.a.C18.2
H1
Trp
Thr
Carnosine
lysoPC.a.C18.0
PC.aa.C40.5
*Gly
Tyr
Histamine
lysoPC.a.C16.1
C0
His
Ac.Orn
PC.aa.C32.2
PC.aa.C34.3
PC.ae.C40.3
PC.ae.C38.0
lysoPC.a.C26.1
SM.C26.1
Ser
Lys
Asn

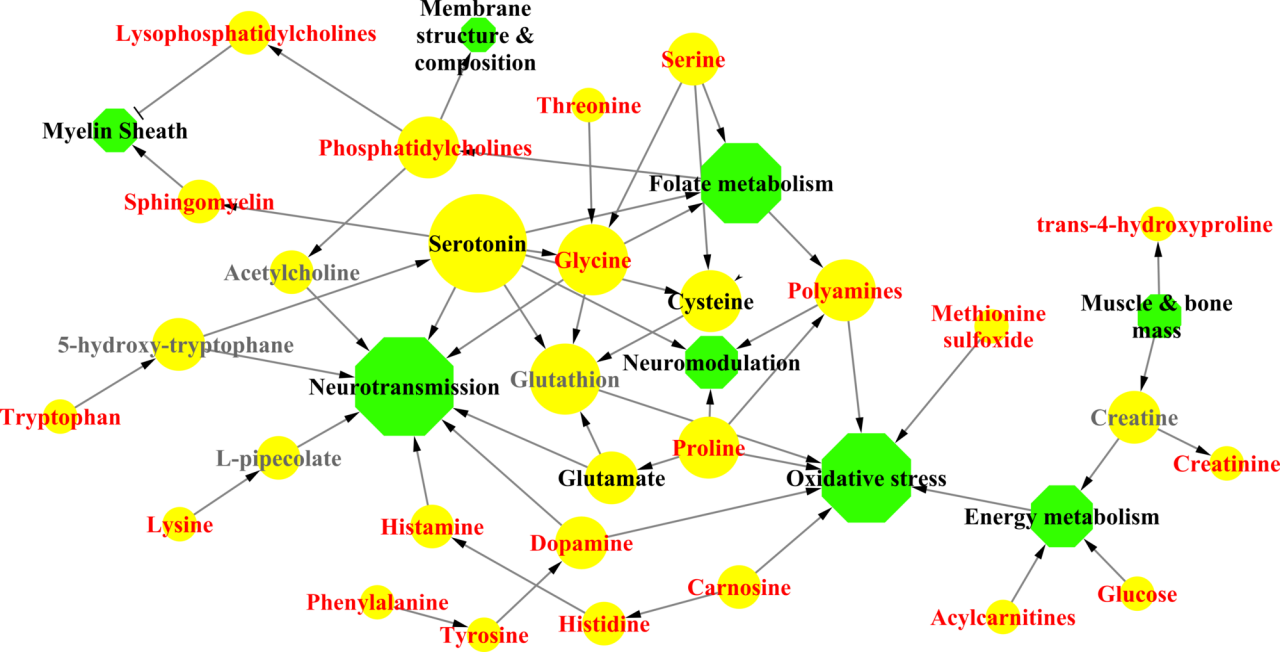
Lysophosphatidylcholines
Membrane structure & composition
Serine
Threonine
Myelin Sheath
Phosphatidylcholines
Folate metabolism
Sphingomyelin
Serotonin
Glycine
trans-4-hydroxyproline
Acetylcholine
Cysteine
Polyamines
Muscle & bone mass
Methionine sulfoxide
5-hydroxy-tryptophane
Neuromodulation
Neurotransmission
Glutathion
Tryptophan
Creatine
Creatinine
L-pipecolate
Proline
Glutamate
Oxidative stress
Energy metabolism
Lysine
Histamine
Dopamine
Carnosine
Glucose
Phenylalanine
Histidine
Acylcarnitines
Tyrosine